Published in IET Microwaves, Antennas & Propagation
Received on 19th February 2009
Revised on 2nd July 2009
doi: 10.1049/iet-map.2009.0057

ISSN 1751-8725

Physical modelling of multiple-input multiple-output antennas and channels by means of the spherical vector wave expansion

A.A. Glazunov[1,*] *M. Gustafsson*[1] *A.F. Molisch*[2,†]
F. Tufvesson[1]

[1]*Centre for Wireless Network Design, University of Bedfordshire, Park Square, Luton, LU1 3JU, UK*
[2]*Department of Electrical Engineering, University of Southern California, Los Angeles, CA, USA*
[*]*At the time of this work, A.A. Glazunov was with the Department of Electrical and Information Technology, Lund University, Box 118, Lund SE-221 00, Sweden*
[†]*At the time of this work, A.F. Molisch was with Mitsubishi Electric Research Labs, Cambridge, MA, USA, and Department of Electrical and Information Theory, Lund University, Lund, Sweden*
E-mail: alayon.glazunov@gmail.com

Abstract: The authors propose a new physically motivated model that allows the study of the interaction between the antennas and the propagation channel for multiple-input multiple-output (MIMO) systems. The key tools employed in the model are the expansion coefficients of the electromagnetic field in spherical vector waves and the scattering matrix representation of the properties of the antenna. The authors derive the expansion of the MIMO channel matrix, $\boldsymbol{H}$, in spherical vector wave modes of the electromagnetic field of the antennas as well as the propagation channel. The authors also introduce the channel scattering dyadic, $\mathcal{C}$, with a corresponding correlation model for co-polarised and cross-polarised elements and introduce the concept of mode-to-mode channel mapping, the $\boldsymbol{M}$-matrix, between the receive and transmit antenna modes. The $\boldsymbol{M}$-matrix maps the modes excited by the transmitting antenna to the modes exciting the receive antennas and vice versa. The covariance statistics of this $\boldsymbol{M}$-matrix are expressed as a function of the double-directional power-angular spectrum (PAS) of co-polarised and cross-polarised components of the electromagnetic field. Their approach aims at gaining insights into the physics governing the interaction between antennas and channels and it is useful for studying the performance of different antenna designs in a specified propagation channel as well as for modelling the propagation channel. It can furthermore be used to quantify the optimal properties of antennas in a given propagation channel. The authors illustrate the developed methodology by analysing the interaction of a 2×2 system of slant polarised half-wavelength dipole antennas with some basic propagation channel models.

1 Introduction

In the last two decades, communication systems with multi-port antenna systems at both the receiver and the transmitter, multiple-input multiple-output (MIMO) systems, have attracted much attention [1–6]. These systems have the potential to provide higher bandwidth efficiency and greater robustness to fading in wireless systems because of their intrinsic ability to exploit the spatial and polarisation domains. The antennas are fundamental elements of the physical layer and play an essential role in maximising system performance for a given propagation channel. Therefore a thorough understanding of the physics of the interaction between the antennas and the propagation channel is essential for analysing and optimising MIMO systems.

The first theoretical investigations of MIMO systems [1–3] were based on the transfer function matrix, the

$\boldsymbol{H}$-matrix, which contains as its elements the transfer function from each transmit antenna element (More specifically, from each transmit antenna connector to each receive antenna connector.) to each receive antenna element and therefore lumps the antenna properties together with the propagation channel. This approach does not allow studying the antenna–channel interaction and the antenna array optimisation. To alleviate this problem, Steinbauer et al. [7] introduced the 'double-directional channel model' that describes the 'directions-of-departure' (DoD) and 'directions-of-arrival' (DoA) of the multi-path components (MPCs) or plane waves. Although this expansion has been used extensively in the past, for example, [8–10] and is 'natural' for propagation models, it is not compact (i.e. can require a large number of terms) and does not give straightforward insights of the interaction of channels especially with small antennas. We are therefore interested in an alternative, compact and physically tractable description of the joint properties of channels and antennas.

Fortunately, both the propagation channel and the antennas can be described in terms of the electromagnetic field and thus a homogeneous characterisation is feasible. More precisely, it is possible to use the expansion of the electromagnetic field in spherical vector waves [11], together with the scattering matrix representation of an antenna [12] to get a unified description. It is worthwhile to notice that all properties of multi-port antennas can be derived from the scattering matrix representation [12], inclusive mutual coupling between antenna elements of the same multi-port antenna and/or between the antennas belonging to different antenna systems and spatially separated as outlined in [13]. The spherical vector wave expansion is a natural way to express the polarisation, angle and spatial properties of MIMO systems. By expressing the channel directly in the spherical vector wave modes [14], it is possible to determine the characteristics of a multi-port antenna system for wireless transmission of information, in that same propagation channel. Our goal is to formulate a theoretical framework to study the mechanisms governing the interaction between antennas and channels in order to determine the optimum information transmission over wireless channels with multi-port antenna systems.

Previous theoretical studies employed spherical modes to represent the propagation channel in terms of scalar fields, see for example, [15–22]. However, the physics of electromagnetic fields is naturally described in terms of vector fields, where the polarisation plays an important role. The application of the spherical vector wave expansion of electromagnetic waves as well as the modal expansion in guiding structures for deterministic MIMO channels has been intuitively outlined in [23]. There some initial insights into the electromagnetic MIMO channel capacity are also provided. A characterisation of the diversity performance of antennas with multiple elements in terms of cross-correlation using spherical eigenmodes was presented [24]. We recently introduced the spherical vector wave mode expansion of the field and the scattering matrix representation of the antenna to quantify the interaction between the antennas and the propagation channel in a more physically meaningful way. For example in [25–27], we studied the spectral efficiency of MIMO antennas based on antenna theory and broadband matching theory in the isotropic channel (or 3D uniform channel). In [14], our focus was on the spatio-polar characterisation of an arbitrary receive multi-port antenna in a random electromagnetic field. However, the physics of the interaction between receive antennas, the transmit antennas, and the propagation channel in MIMO systems was not addressed in previous research. In this work, we extend the framework for analysis of antenna–channel interaction to MIMO channels and multi-port antenna systems at Tx and Rx. This is accomplished by expressing both the stochastic channel and deterministic antennas in a unified way. The main contributions of the paper can be summarised as follows:

1. We introduce the concept of mode-to-mode channel matrix, the $\boldsymbol{M}$-matrix, to describe the coupling between the modes excited by the transmit and the receive antennas. The $\boldsymbol{M}$-matrix contains all relevant information about the channel on a fundamental level, information about the spherical vector wave modes that are the most likely to be excited by the propagation channel. The $\boldsymbol{M}$-matrix also provides a mapping of modes excited at the receiver and transmitter, respectively.

2. Using the correlation model for the amplitudes incident at the receive antenna [14], we derive a general correlation model for the double-directional channel. More specifically, we study the correlation between the components of the channel scattering dyadic $\boldsymbol{\mathcal{C}}$. (This is basically the double-directional channel transfer function introduced in [7] in combination with the physical representation in [28].) The dyadic $\boldsymbol{\mathcal{C}}$ maps the field radiated by the transmitting antenna to that impinging at the receive antenna by superposition of plane waves. (This is a good approximation when both transmitting and receiving antennas are in each others' far-field region as well as when the distance from the antennas to the scatterers are much larger than the size of the scatterers. This approximation is required for the scattering approach assumed in this paper.) We show that the formulation is equivalent to the single-scatterer process, where the scatterer represents the propagation channel. (It is worthwhile to notice that this equivalence only holds in the narrowband case.)

3. We expand the channel transfer function matrix, the $\boldsymbol{H}$-matrix, in spherical vector wave modes, that is, the $\boldsymbol{M}$-matrix, using the derived correlation model for the elements of the channel scattering dyadic. We also provide results for first- and second-order statistics of the expansion coefficients based on the assumption that the dyadic elements are independently distributed Gaussian variables.

The derived equations allow us to establish a relationship between $\boldsymbol{H}$ and $\boldsymbol{M}$, and therefore to describe the spatial,

doi: 10.1049/iet-map.2009.0057

directional and polarisation properties of the channel and the antennas for MIMO systems in spherical vector waves.

The remainder of the paper is organised as follows. In Section 2, we present a brief introduction to the spherical vector wave expansion of the electromagnetic field and the antenna scattering matrix. Here we also introduce the $\boldsymbol{M}$-matrix concept. Section 3 introduces the channel scattering dyadic, $\mathcal{C}$, and some of its properties, and derives a model for the correlation between the dyadic components. In Section 4, we provide the expansion of the channel matrix $\boldsymbol{H}$ in spherical vector waves. We further show some properties of the expansion coefficients and provide a brief discussion with some specific examples. Section 5 provides simulation results for a 2×2 MIMO slant-antenna polarisation system with half-wavelength dipoles orthogonally placed with respect to each other, in a generic propagation channel. Finally, a summary with conclusions is in given Section 6.

2 Mode-to-mode MIMO channel matrix, *M*

In this section, we present a straightforward treatment that aims at interconnecting the signals from the receive antenna, the field from the transmit antenna and the field impinging at the receive antenna. Building on the approach of [14], we define two main mathematical tools that describe the interaction between antennas and channels. This approach provides a complete description of reciprocal antennas by using the scattering matrix of the antennas of each multi-port antenna system involved in the communications.

Consider two multi-port antennas separated by a distance d as shown in Fig. 1 where one of them acts as a transmitter (Tx) and one acts as a receiver (Rx). Further assume that each antenna phase center coincides with the origin of their own coordinate system and that there is no mutual coupling between the Tx and Rx antennas (This is fulfilled when d is larger than a few wavelengths, that is, in most practically relevant cases.) though we do allow for mutual coupling between the elements of the TX antenna (and similarly for the RX antenna).

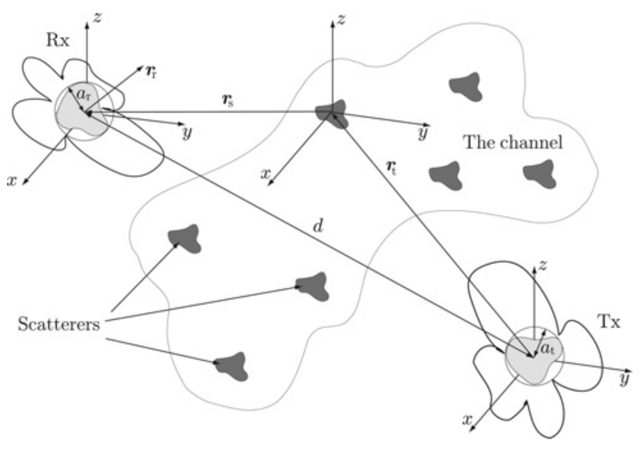

Figure 1 *Schematic representation of the propagation channel with non-interacting scatterers and the antennas*

The electric field emitted by the Tx antenna, $\boldsymbol{E}^{(t)}(\boldsymbol{r}_t)$, can be expanded into outgoing spherical vector waves $\boldsymbol{u}_\kappa^{(2)}(k\boldsymbol{r}_t)$, where $\boldsymbol{r}_t$ is the coordinate vector with origin in the phase centre of the Tx and $\kappa \to (\tau, m, l)$ is a multi-index that is also calculated as $\kappa = 2(l^2 + l - 1 + m) + \tau$, for $l = 1 \ldots l_{\max}$, $m = -l \ldots l$ and $\tau = 1, 2$, see Appendices A and B in [29]. Then, the expansion of the transmitted electric field in a source-free region (all sources are inside the sphere with radius a_t) [11] can be expressed as

$$\boldsymbol{E}^{(t)}(\boldsymbol{r}_t) = k\sqrt{2\eta}\sum_\kappa b_\kappa \boldsymbol{u}_\kappa^{(2)}(k\boldsymbol{r}_t) \quad \text{for } |\boldsymbol{r}_t| \geq a_t \tag{1}$$

where η is the free-space impedance, k is the wave-number and the b_κ are the expansion coefficients. Similarly, the electric field sensed by the receive antenna, $\boldsymbol{E}^{(r)}(\boldsymbol{r}_r)$, can be expanded in incoming spherical vector waves $\boldsymbol{u}_\iota^{(1)}(k\boldsymbol{r}_r)$

$$\boldsymbol{E}^{(r)}(\boldsymbol{r}_r) = k\sqrt{2\eta}\sum_\iota a_\iota \boldsymbol{u}_\iota^{(1)}(k\boldsymbol{r}_r) \quad \text{for } |\boldsymbol{r}_r| \geq a_r \tag{2}$$

where $\iota \to (t, \mu, \lambda)$ is the multi-index notation for the Rx antenna, which is computed as $\iota = 2(\lambda^2 + \lambda - 1 + \mu) + t$.

The scattering matrix of an N-port antenna provides a full description of all its properties [12], that is, the incoming signals, $\boldsymbol{v} \in \boldsymbol{C}^{N\times 1}$ and waves, $\boldsymbol{a} \in \boldsymbol{C}^{\infty\times 1}$, the outgoing signals, $\boldsymbol{w} \in \boldsymbol{C}^{N\times 1}$ and waves $\boldsymbol{b} \in \boldsymbol{C}^{\infty\times 1}$, the matrix containing the complex antenna reflection coefficients, $\Gamma \in \boldsymbol{C}^{N\times N}$, the matrix containing the antenna receiving coefficients, $\boldsymbol{R} \in \boldsymbol{C}^{N\times\infty}$, the matrix containing the antenna transmitting coefficients, $\boldsymbol{T} \in \boldsymbol{C}^{\infty\times N}$ and the matrix containing the antenna scattering coefficients $\boldsymbol{S} \in \boldsymbol{C}^{\infty\times\infty}$ [12].

$$\begin{pmatrix} \Gamma & \boldsymbol{R} \\ \mathrm{T} & \boldsymbol{S} \end{pmatrix}\begin{pmatrix} \boldsymbol{v} \\ \boldsymbol{a} \end{pmatrix} = \begin{pmatrix} \boldsymbol{w} \\ \boldsymbol{b} \end{pmatrix} \tag{3}$$

From here and on, we will use the term scattering matrix to denote different mathematical objects, whose meaning will follow from the context. Based on the spherical wave expansion above and the scattering matrix representation of the antenna, we know that a transmitting antenna is characterised by $\boldsymbol{a} = 0$ and $\boldsymbol{w} = 0$. It is worthwhile to notice that transmit and the receive antennas are each characterised by a scattering matrix (see (3)), though with different parameters. Moreover, we use the same notation for both the transmit and receive antennas. However, throughout the paper, $\boldsymbol{a}, \boldsymbol{w}, \boldsymbol{R}$ and $\boldsymbol{b}, \boldsymbol{v}, \boldsymbol{T}$ are used to identify the receive and transmit antennas, respectively. Consequently, the transmitted signals, $\boldsymbol{v}$, are mapped into the outgoing spherical vector wave expansion coefficients,

doi: 10.1049/iet-map.2009.0057

$\boldsymbol{b}$, by the transmission matrix, $\boldsymbol{T}$, as

$$\boldsymbol{b} = \boldsymbol{T}\boldsymbol{v} \tag{4}$$

On the other hand, at the receiving side, setting $\boldsymbol{b} = 0$ and $\boldsymbol{v} = 0$, the incoming spherical vector wave expansion coefficients, $\boldsymbol{a}$, are mapped into the received signals, $\boldsymbol{w}$, through the antenna matrix, $\boldsymbol{R}$, as

$$\boldsymbol{w} = \boldsymbol{R}\boldsymbol{a} \tag{5}$$

In order to establish a relationship between input–output signals at the transmit and the receive antennas, that is, transmitted signals, $\boldsymbol{v}$, and received signals, $\boldsymbol{w}$, we need first to establish a mapping between the outgoing waves at the transmit antennas, $\boldsymbol{b}$ and the incoming waves at the receive antenna, $\boldsymbol{a}$. We do this by using a mode-to-mode mapping $\boldsymbol{M}$ [26]

$$\boldsymbol{a} = \boldsymbol{M}\boldsymbol{b} \tag{6}$$

The mode-to-mode MIMO channel matrix, $\boldsymbol{M}$, is a stochastic matrix that describes the properties of the wireless channel in terms of the multimode expansion coefficients of the electromagnetic field. Hence, combining (4)–(6), we arrive at the following linear relationship for the MIMO channel

$$\boldsymbol{w} = \boldsymbol{R}\boldsymbol{M}\boldsymbol{T}\boldsymbol{v} \tag{7}$$

Denoting the MIMO channel transfer function by

$$\boldsymbol{H} = \boldsymbol{R}\boldsymbol{M}\boldsymbol{T} \tag{8}$$

we then arrive at the classical model for the input–output relation between the transmitted, $\boldsymbol{x} = \boldsymbol{v}$, and the received signals in a noisy channel, $\boldsymbol{y} = \boldsymbol{w} + \boldsymbol{n}$

$$\boldsymbol{y} = \boldsymbol{H}\boldsymbol{x} + \boldsymbol{n} \tag{9}$$

where $\boldsymbol{n}$ is the additive white Gaussian noise (AWGN) component.

Expressions (4)–(9) establish a full chain of relationships that enables the analysis of the interaction between the antennas and the propagation channel and their impact on the communication link by simple relationships. The classical transfer function matrix $\boldsymbol{H}$ is a linear function of the physical properties of both the antennas, $\boldsymbol{R}$ and $\boldsymbol{T}$ and the propagation channel $\boldsymbol{M}$.

3 Channel scattering $\mathcal{C}$-dyadic

In the previous section, we introduced a mapping, the $\boldsymbol{M}$-matrix, between the modes excited by the transmit antennas to the modes excited by the receive antenna. The spatio-polar selectivity nature of the wireless propagation channels has been extensively investigated for stochastic propagation channels, we know therefore that the properties of the $\boldsymbol{M}$-matrix should be a function of the polarimetric double-directional impulse response (if we are considering a single, deterministic, channel) or the power angular spectrum (PAS) of each of the orthogonal polarisations of the electromagnetic waves, as well as the depolarisation of transmitted waves. The dependence of the $\boldsymbol{M}$-matrix on the propagation channel need to be studied experimentally to fully establish its properties.

In the following, we show from first principles, that the multiple-scattering processes taking place in the wireless propagation channel can be described by a scattering dyadic. Its representation is similar to the scattering dyadic when only a single-scattering process is considered. This is of course an effective (or equivalent) description of the actual scattering process since multiple-scattering actually takes place within this effective scatterer, that is, the channel. Backscattering from the channel to the transmitting antenna as well as from the receiving antenna to the channel is neglected. Hence, we can model the channel with a 'black box' where the energy that is transmitted in direction $\hat{\boldsymbol{k}}_{\mathrm{t}}$ (the symbol $(\hat{.})$ denotes a unit vector) traverses the channel by means of an arbitrary number of interactions with physical objects (the interactions may be because of scattering, specular reflection, diffraction and others) and arrives at the receiver from one or multiple directions $\hat{\boldsymbol{k}}_{\mathrm{r}}$. In the following, we first derive some properties of the $\boldsymbol{M}$-matrix for some special cases (only one scatterer present; only single-scattering processes), and then give a more general description.

Consider now the situation where there is a single linear scatterer present at a position in space defined by the radius-vector $\boldsymbol{r}_{\mathrm{t}}$ defined in the coordinate system of the Tx antenna, see Fig. 7. The field radiated by the transmitting antenna port j, $\boldsymbol{E}_j(\boldsymbol{r}_{\mathrm{t}})$, is defined in the far-field region by the far-field amplitude, $\boldsymbol{F}_j(\hat{\boldsymbol{r}}_{\mathrm{t}})$ radiated in direction $\hat{\boldsymbol{r}}_{\mathrm{t}} = \mathbf{r}_{\mathrm{t}}/r_{\mathrm{t}}$

$$\boldsymbol{E}_j(\boldsymbol{r}_{\mathrm{t}}) = \boldsymbol{F}_j(\hat{\boldsymbol{r}}_{\mathrm{t}})\frac{\mathrm{e}^{-\mathrm{i}kr_{\mathrm{t}}}}{kr_{\mathrm{t}}} + \mathcal{O}(r_{\mathrm{t}}^{-2}) \quad \text{as } r_{\mathrm{t}} \to \infty \tag{10}$$

where $\mathcal{O}(x^n)$ is the 'big-O' notation standing for 'order of' asymptotics, that is, $|\mathcal{O}(x^n)/x^n| < C$ as $x \to \infty$ and $r_{\mathrm{t}} = |\boldsymbol{r}_{\mathrm{t}}|$.

An electric field $\boldsymbol{E}_j$ impinges on a scatterer from direction $\hat{\boldsymbol{r}}_{\mathrm{t}}$. In the far-field region, the scattered electric field $\boldsymbol{E}_{\mathrm{s}}$ is fully described by the far-field amplitude $\boldsymbol{F}_{\mathrm{s}}$ scattered in direction $\hat{\boldsymbol{r}}_{\mathrm{s}} = \boldsymbol{r}_{\mathrm{s}}/r_{\mathrm{s}}$ as

$$\boldsymbol{E}_{\mathrm{s}}(\boldsymbol{r}_{\mathrm{s}}) = \boldsymbol{F}_{\mathrm{s}}(\hat{\boldsymbol{r}}_{\mathrm{s}})\frac{\mathrm{e}^{-\mathrm{i}kr_{\mathrm{s}}}}{kr_{\mathrm{s}}} + \mathcal{O}(r_{\mathrm{s}}^{-2}) \quad \text{as } r_{\mathrm{s}} \to \infty \tag{11}$$

where $\boldsymbol{F}_{\mathrm{s}}$ can be expressed in terms of the scattering dyadic $\mathcal{S}(\hat{\boldsymbol{r}}_{\mathrm{s}}, \hat{\boldsymbol{r}}_{\mathrm{t}})$

$$\boldsymbol{F}_{\mathrm{s}}(\hat{\boldsymbol{r}}_{\mathrm{s}}) = \mathcal{S}(\hat{\boldsymbol{r}}_{\mathrm{s}}, \hat{\boldsymbol{r}}_{\mathrm{t}}) \cdot \boldsymbol{E}_j(\boldsymbol{r}_{\mathrm{t}}) \tag{12}$$

where we have assumed that the amplitude of the plane wave incident at the scatterer from direction $\hat{\boldsymbol{r}}_{\mathrm{t}}$ is given by $\boldsymbol{E}_j(\boldsymbol{r}_{\mathrm{t}})$.

doi: 10.1049/iet-map.2009.0057

Hence, from (10)–(12), the scattered field can be expressed as

$$\boldsymbol{E}_s(\boldsymbol{r}_s) \simeq \mathcal{S}(\hat{\boldsymbol{r}}_s, \hat{\boldsymbol{r}}_t) \cdot \boldsymbol{F}_j(\hat{\boldsymbol{r}}_t) \frac{e^{-ik(r_s+r_t)}}{k^2 r_s r_t} \quad \text{as } r_s, r_t \to \infty \tag{13}$$

In the far-field region the properties of the field are those of a plane wave, therefore the scattered field in the far-field region can be described by a plane wave

$$\boldsymbol{E}_s(\boldsymbol{r}_r) \simeq \boldsymbol{E}_0 \, e^{-ik\hat{\boldsymbol{r}}_s \cdot \boldsymbol{r}_r} \tag{14}$$

with the complex amplitude given by

$$\boldsymbol{E}_0 = \frac{e^{-ikr_s}}{kr_s} \mathcal{S}(\hat{\boldsymbol{r}}_s, \hat{\boldsymbol{r}}_t) \cdot \boldsymbol{E}_j(\boldsymbol{r}_t) \tag{15}$$

In wireless communications channels, it is seldom the case that there is only a single scatterer interacting with the receive and transmit antennas. Many scatterers have to be considered in order to completely define the propagation channel. This is hard due to the fact that multiple-scattering propagation that takes place and the shape and electromagnetic properties of each scatterer are not exactly known. However, in many applications the exact physical properties of the channel scatterers are superfluous. Rather, we are mainly concerned with the statistical description of the channel, which is a widely used approach [8, 30, 31]. Of course, if there are scatterers in the near-field region of the antenna this assumption is not valid. For a handheld terminal the user's head, hands or body will in general have a large impact on the performance. Similarly, for a base station scenario structures surrounding the base station antenna will affect its radiation pattern.

We next consider a situation where many scatterers are present between the transmit and the receive antennas. We assume that (i) all the scatterers are in the far-field regions of both the receiver and the transmitter and (ii) scatterers are grouped such that the maximum dimensions of a group of scatterers is much smaller than the distances to both the receiver and the transmitter. The definition of a group of scatterers here is related to both the classical definition of a cluster and the concept of multipath groups. However, strictly speaking it does not fit either of them. A thorough description of both cluster and multipath group concepts can be found in [10, 32, 33].

It can be shown that, if assumption (ii) holds, then the scattered field $\boldsymbol{E}_s$ can be written in a similar way as the single-scatterer case (12)–(13), where the effective scattering dyadic $\mathcal{S}_c^e(\hat{\boldsymbol{k}}_r, \hat{\boldsymbol{k}}_t)$ replaces $\mathcal{S}$ for each group of scatterers. Observe that in order to introduce a more general framework we from now on express the directionality of the channels an the antennas in terms of wave vectors, $\hat{\boldsymbol{k}}$, instead of radius vectors $\hat{\boldsymbol{r}}$.

The key difference is that the contributions from the scatterers in each group of scatterers are superimposed, leading to fading – in other words, the field arising from each group of scatterers can be modelled as a stochastic process. We can then express the total scattered far-field as a superposition of the scattered fields from each group of scatterers. Hence, we arrive at the following relationship for $\boldsymbol{E}_s$

$$\boldsymbol{E}_s = \mathcal{C}(\hat{\boldsymbol{k}}_r, \hat{\boldsymbol{k}}_t) \cdot \boldsymbol{F}_j(\hat{\boldsymbol{k}}_t) \tag{16}$$

where $\mathcal{C}(\hat{\boldsymbol{k}}_r, \hat{\boldsymbol{k}}_t)$ is the channel scattering dyadic [7, 28]

$$\mathcal{C}(\hat{\boldsymbol{k}}_r, \hat{\boldsymbol{k}}_t) = \sum_c \frac{e^{-ik(r_{rc}+r_{tc})}}{k^2 r_{rc} r_{tc}} \mathcal{S}_c^e(\hat{\boldsymbol{k}}_r, \hat{\boldsymbol{k}}_t) \tag{17}$$

where the summation is over the group of scatterers, r_{rc} and r_{tc} are the distances between a reference position within the group of scatterers and the receiver and the transmitter, respectively.

Since the scattering process is assumed to be linear, it follows that for reciprocal channels, $\mathcal{C}(\hat{\boldsymbol{k}}_r, \hat{\boldsymbol{k}}_t)$ satisfies the identity (see Appendix E in [29] for further reference)

$$\mathcal{C}(\hat{\boldsymbol{k}}_r, \hat{\boldsymbol{k}}_t) = \mathcal{C}^T(-\hat{\boldsymbol{k}}_t, -\hat{\boldsymbol{k}}_r) \tag{18}$$

As a result of the assumptions made, one can further state that the received field, that is, the field incident at the receiver can be obtained as a linear transformation of the transmitted field. Components of the electric field generated by the transmitter antenna and the electric field available at the receiver are connected through a matrix that could be interpreted as a 'scattering' dyadic $\mathcal{C}(\hat{\boldsymbol{k}}_r, \hat{\boldsymbol{k}}_t)$, which is basically the channel transfer function in the 'angular domain' $(\hat{\boldsymbol{k}}_r, \hat{\boldsymbol{k}}_t)$, or equivalently, the double-directional impulse response or transfer function [7, 8].

It is worthwhile to observe that the superposition of the scattered fields from different group of scatterers is true only when there is no interaction or coupling between each group of scatterers; in reality the coupling between groups of scatterers always exists. This is an interesting question that needs further investigations, but it is outside the scope of this paper.

3.1 Correlation model for the channel scattering dyadic, $\mathcal{C}$

In order to further study the statistical properties of the $\boldsymbol{M}$-matrix, we need to introduce a correlation model for co-polarised and cross-polarised elements of the channel scattering dyadic. We write the stochastic matrix $\mathcal{C}(\hat{\boldsymbol{k}}_r, \hat{\boldsymbol{k}}_t)$ as

$$\mathcal{C}(\hat{\boldsymbol{k}}_r, \hat{\boldsymbol{k}}_t) = \begin{pmatrix} \mathcal{C}_{\theta\theta} & \mathcal{C}_{\theta\phi} \\ \mathcal{C}_{\phi\theta} & \mathcal{C}_{\phi\phi} \end{pmatrix} \tag{19}$$

where $\mathcal{C}_{\theta\theta}$ and $\mathcal{C}_{\phi\phi}$ are co-polarised components, $\mathcal{C}_{\theta\phi}$ and $\mathcal{C}_{\phi\theta}$ are the cross-polarised components, with θ and ϕ

doi: 10.1049/iet-map.2009.0057

denoting two orthogonal polarisations. We further postulate that each entry of $\mathcal{C}(\hat{\boldsymbol{k}}_r, \hat{\boldsymbol{k}}_t)$ is a zero-mean complex Gaussian variable

$$\langle \mathcal{C}_{\alpha\beta} \rangle = 0 \tag{20}$$

where $\alpha = \{\theta, \phi\}$ and $\beta = \{\theta, \phi\}$ and $\langle \cdot \rangle$ denote the ensemble average (see, e.g. [34], p. 285). The Gaussian assumption is valid if the number of scatterers in each group of scatterers is large and none of them are dominating [33].

The cross-covariance is given by

$$\langle \mathcal{C}_{\alpha\beta} \mathcal{C}^*_{\alpha'\beta'} \rangle = \mathcal{P}_{\alpha\beta}(\hat{\boldsymbol{k}}_r, \hat{\boldsymbol{k}}_t) \delta^2(\hat{\boldsymbol{k}}_r - \hat{\boldsymbol{k}}'_r) \delta^2(\hat{\boldsymbol{k}}_t - \hat{\boldsymbol{k}}'_t) \delta_{\alpha\alpha'} \delta_{\beta\beta'} \tag{21}$$

where $\delta^2(\hat{\boldsymbol{k}}) = \delta(\theta)\delta(\phi)/\sin(\theta)$ denotes the Dirac-delta in spherical coordinates defined on the sphere of unit radius, the asterisk $(.)^*$ denotes complex conjugate and $\mathcal{P}_{\alpha\beta}(\hat{\boldsymbol{k}}_r, \hat{\boldsymbol{k}}_t)$ denotes the double-directional power angular spectrum (DD-PAS) between polarisation α at the receiver and polarisation β at the transmitter. See, for example [7, 9, 35, 36] for further details on the DD-PAS.

The DD-PAS of both co-polarised and cross-polarised components can be expressed in terms of joint probability distributions of the angle of arrivals (AoAs) and angle of departures (AoDs) following the convention presented in [14]

$$\mathcal{P}_{\alpha\beta}(\hat{\boldsymbol{k}}_r, \hat{\boldsymbol{k}}_t) = P_{\alpha\beta} p_{\alpha\beta}(\hat{\boldsymbol{k}}_r, \hat{\boldsymbol{k}}_t) \tag{22}$$

where $P_{\alpha\beta}$ denotes the co- or cross-coupling power between polarisations along α and β. The joint probability density function $p_{\alpha\beta}(\hat{\boldsymbol{k}}_r, \hat{\boldsymbol{k}}_t)$ satisfies the normalisation

$$\int\int p_{\alpha\beta}(\hat{\boldsymbol{k}}_r, \hat{\boldsymbol{k}}_t) \, d\Omega_r \, d\Omega_t = 1 \tag{23}$$

Hence, $P_{\alpha\beta} = \int\int \mathcal{P}_{\alpha\beta}(\hat{\boldsymbol{k}}_r, \hat{\boldsymbol{k}}_t) \, d\Omega_r \, d\Omega_t$, where we have expressed $\mathcal{P}_{\alpha\beta}(\hat{\boldsymbol{k}}_r, \hat{\boldsymbol{k}}_t)$ in spherical coordinates.

The covariance model (21) is, as we show in Appendix C in [29], a direct consequence of the correlation model for the incident field presented in [14] and the reciprocity of the wireless propagation channel. Here, for the sake of clarity, we restrict our analysis to the Rayleigh fading environment. Extension to the more general Rice case is straightforward following the exposition presented here and in [14]. The main assumptions for the model of the Rayleigh case are

1. The phases of the co-polarised waves are independent for different DoAs $\hat{\boldsymbol{k}}$ and $\hat{\boldsymbol{k}}'$.

2. The phases of the cross-polarised waves are independent for any DoAs $\hat{\boldsymbol{k}}$ and $\hat{\boldsymbol{k}}'$.

Note that these assumptions are a straightforward generalisation of the generalised wide sense stationary uncorrelated scattering (WSSUS) assumption [37, 38].

Let E_α, E'_β denote the complex amplitudes of the random incident electric field in α and β polarisations, respectively, and $\tilde{E}_\alpha$ and $\tilde{E}_\beta$ denote the corresponding components of the plane wave spectrum, then we summarise the above postulates

$$\langle \tilde{E}_\alpha \tilde{E}'^*_\beta \rangle = \langle E_\alpha E^*_\alpha \rangle \delta^2(\hat{\boldsymbol{k}} - \hat{\boldsymbol{k}}') \delta_{\alpha\beta} \tag{24}$$

where $\delta_{\alpha\beta}$ denotes the Kronecker-delta function.

For the characterisation, we also need the cross-polarisation ratio (XPR) that characterises the power imbalance between the two orthogonal polarisations. It is defined as the ratio between the power in the θ-polarisation and the power in the ϕ-polarisation

$$\chi = \frac{P_{\theta\theta} + P_{\theta\phi}}{P_{\phi\theta} + P_{\phi\phi}} \tag{25}$$

where the power of the co-polarised and cross-polarised components have been defined above. In many practical cases, $P_{\theta\phi} \simeq P_{\phi\theta} \ll P_{\theta\theta}, P_{\phi\phi}$ and the XPR reduces to $\chi = P_{\theta\theta}/P_{\phi\phi}$.

4 Spherical vector wave expansion of the double-directional MIMO channel

Our main focus now is to derive the correlation properties of the mode-to-mode channel, the $\boldsymbol{M}$-matrix, given the PAS of the double-directional channel. The incident field can be described in either plane waves or spherical vector waves. This section gives the transformation between the two.

The expansion of an arbitrary electromagnetic field $\boldsymbol{E}(\boldsymbol{r})$ at the observation point in space $\boldsymbol{r}$ in regular spherical vector waves, $\boldsymbol{v}_\iota(k\boldsymbol{r})$ (see Appendix A in [29]) can be written as

$$\boldsymbol{E}(\boldsymbol{r}) = k\sqrt{2\eta} \sum_\iota f_\iota \boldsymbol{v}_\iota(k\boldsymbol{r}) \tag{26}$$

The expansion coefficients f_ι [14] are given by

$$f_\iota = \frac{4\pi(-\mathrm{i})^{\lambda-\ell+1}}{k\sqrt{2\eta}} \int \boldsymbol{A}^*_\iota(\hat{\boldsymbol{k}}_r) \cdot \tilde{\boldsymbol{E}}_0(\hat{\boldsymbol{k}}_r) \, d\Omega_r \tag{27}$$

where $\tilde{\boldsymbol{E}}_0(\hat{\boldsymbol{k}}_r)$ denotes the amplitude of the (random) complex plane-wave spectrum (PWS) in the direction $\hat{\boldsymbol{k}}_r$, and $\boldsymbol{A}^*_\iota(\hat{\boldsymbol{k}}_r)$ is the complex conjugated spherical vector harmonic with index set $\iota \to \{\tau\mu\lambda\}$. The relationship between the incident field at the antenna and the antenna field of the receiver is given by (5) and (27) as we outlined in [14]. Next we relate the incident field to the transmit field, as given by (4)–(6).

doi: 10.1049/iet-map.2009.0057

Observing that the PWS of the incident field can be obtained from the integral over the AoD, (16)

$$\tilde{\boldsymbol{E}}_0(\hat{\boldsymbol{k}}_\mathrm{r}) = \int \boldsymbol{C}(\hat{\boldsymbol{k}}_\mathrm{r}, \hat{\boldsymbol{k}}_\mathrm{t}) \cdot \boldsymbol{F}_j(\hat{\boldsymbol{k}}_\mathrm{t})\, \mathrm{d}\Omega_\mathrm{t} \tag{28}$$

We further expand the far-field amplitude of the transmit field in spherical vector waves in the corresponding coordinate system

$$\boldsymbol{F}_j(\hat{\boldsymbol{k}}_\mathrm{t}) = k\sqrt{2\eta}\sum_{\tau=1}^{2}\sum_{l=1}^{\infty}\sum_{m=-l}^{l} \mathrm{i}^{l+2-\tau} T_{\kappa j} v_j \boldsymbol{A}_\kappa(\hat{\boldsymbol{k}}_\mathrm{t}) \tag{29}$$

By combining (27)–(29), we arrive at the following expression for the expansion coefficients of the incoming field in regular spherical vector waves, $f_{\iota j}$

$$f_{\iota j} = 4\pi \sum_{\kappa}^{\infty} \mathrm{i}^{1+l-\lambda-\tau+t} \ldots \iint \boldsymbol{A}_\iota^*(\hat{\boldsymbol{k}}_\mathrm{r}) \cdot \boldsymbol{C}(\hat{\boldsymbol{k}}_\mathrm{r}, \hat{\boldsymbol{k}}_\mathrm{t}) \cdot \boldsymbol{A}_\kappa(\hat{\boldsymbol{k}}_\mathrm{t}) T_{\kappa j} v_j\, \mathrm{d}\Omega_\mathrm{r}\, \mathrm{d}\Omega_\mathrm{t} \tag{30}$$

where the index j denotes the contribution from the corresponding port at the transmit antenna.

The expansion coefficients $a_{\iota j}$ of the incoming waves are related to the expansion coefficients $f_{\iota j}$ of the regular waves with multipole index ι as

$$2a_{\iota j} = f_{\iota j} \tag{31}$$

This result follows from the properties of the spherical vector wave functions and the fact that the outgoing and incoming waves carry the same power in free space (empty minimal sphere), that is, $\|\boldsymbol{a}\|_F^2 = \|\boldsymbol{b}\|_F^2$, where the scattering matrix $\boldsymbol{S} = \boldsymbol{I}$. Thus, combining (5), (30) and (31), we arrive at the following expression

$$H_{ij} = 2\pi \iint \sum_{\iota}\sum_{\kappa} \mathrm{i}^{1+l-\lambda-\tau+t} \ldots R_{i\iota} \boldsymbol{A}_\iota^*(\hat{\boldsymbol{k}}_\mathrm{r}) \cdot \boldsymbol{C}(\hat{\boldsymbol{k}}_\mathrm{r}, \hat{\boldsymbol{k}}_\mathrm{t}) \cdot \boldsymbol{A}_\kappa(\hat{\boldsymbol{k}}_\mathrm{t}) T_{\kappa j}\, \mathrm{d}\Omega_\mathrm{r}\, \mathrm{d}\Omega_\mathrm{t} \tag{32}$$

This expression describes the mapping of the outgoing (output) signal from the receive antenna port i and the incoming (input) signals at the transmit antenna port j. Hence, (32) is the expansion of the transfer function matrix, $\boldsymbol{H}$, in spherical vector waves under the assumptions provided above. The elements of the channel matrix H_{ij} can also be expressed by expanding (8) in terms of the elements of matrices $R_{i\iota}$, $M_{\iota\kappa}$ and $T_{\kappa j}$

$$H_{ij} = \sum_{\iota}\sum_{\kappa} R_{i\iota} M_{\iota\kappa} T_{\kappa j} \tag{33}$$

where $M_{\iota\kappa}$ are the elements of the matrix coupling the spherical vector wave modes at the receiver $\iota \to (t, \mu, \lambda)$ and the transmitter $\kappa \to (\tau, m, l)$, respectively. Now, by comparing (32) and (33), we obtain that $M_{\iota\kappa}$ is given by the double integral

$$M_{\iota\kappa} = 2\pi \mathrm{i}^{1+l-\lambda-\tau+t} \ldots \iint \boldsymbol{A}_\iota^*(\hat{\boldsymbol{k}}_\mathrm{r}) \cdot \boldsymbol{C}(\hat{\boldsymbol{k}}_\mathrm{r}, \hat{\boldsymbol{k}}_\mathrm{t}) \cdot \boldsymbol{A}_\kappa(\hat{\boldsymbol{k}}_\mathrm{t})\, \mathrm{d}\Omega_\mathrm{r}\, \mathrm{d}\Omega_\mathrm{t} \tag{34}$$

The entries of the $\boldsymbol{M}$-matrix, that is, the matrix that maps the modes excited at the receiver with the modes excited at the transmitter, are thus directly related to the properties of the channel scattering dyadic $\boldsymbol{C}(\hat{\boldsymbol{k}}_\mathrm{r}, \hat{\boldsymbol{k}}_\mathrm{t})$.

We now proceed to study the statistical properties of the mode-to-mode channel, the $\boldsymbol{M}$-matrix, as well as their implications on the statistics of the 'classical' channel matrix, the $\boldsymbol{H}$-matrix. The elements of the correlation matrix for the entries of the $\boldsymbol{H}$-matrix can be readily obtained from (33) as

$$\mathcal{R}_{ij}^{i'j'} = \sum_{\iota}\sum_{\kappa}\sum_{\iota'}\sum_{\kappa'} R_{i\iota} R_{i'\iota'}^* \mathcal{R}_{\iota\kappa}^{\iota'\kappa'} T_{\kappa j} T_{\kappa' j'}^* \tag{35}$$

where $\mathcal{R}_{ij}^{i'j'} = \langle H_{ij} H_{i'j'}^* \rangle$ denotes the covariance between any two elements of the $\boldsymbol{H}$-matrix, and $\mathcal{R}_{\iota\kappa}^{\iota'\kappa'} = \langle M_{\iota\kappa} M_{\iota'\kappa'}^* \rangle$ denotes the elements of the correlation matrix of the $\boldsymbol{M}$-matrix.

It is worthwhile to notice that (35) contains the full characterisation of the joint correlation properties of the channel and the antennas at both communication link ends. Therefore if $\mathcal{R}_{\iota\kappa}^{\iota'\kappa'}$ is available, or an estimate thereof, we can design the communication system that, for example, maximises the system capacity.

In the following, we study some general properties of the $\boldsymbol{M}$-matrix. The following proposition summarises our main result on the computation of the correlation matrix as function of the PAS of the double-directional channel.

Proposition 1: In a multipath propagation environment characterised by a Gaussian unpolarised field component only (Rayleigh fading), the 'double-directional' expansion coefficients, or the $\boldsymbol{M}$-matrix entries, are Gaussian variates with zero mean, $\langle M_{\iota\kappa} \rangle = 0$, and variance

$$P_{\iota\kappa} = \langle |M_{\iota\kappa}|^2 \rangle = 4\pi^2 \sum_{\alpha}\sum_{\beta} \iint \ldots |A_{\iota,\alpha}(\hat{\boldsymbol{k}}_\mathrm{r})|^2 \mathcal{P}_{\alpha\beta}(\hat{\boldsymbol{k}}_\mathrm{r}, \hat{\boldsymbol{k}}_\mathrm{t}) |A_{\kappa,\beta}(\hat{\boldsymbol{k}}_\mathrm{t})|^2\, \mathrm{d}\Omega_\mathrm{r}\, \mathrm{d}\Omega_\mathrm{t} \tag{36}$$

where the summation is over $\alpha = \{\theta, \phi\}$ and $\beta = \{\theta, \phi\}$. Moreover, the entries of the correlation matrix are functions of the joint power angular spectrum of the co-polarised and

IET Microw. Antennas Propag., 2010, Vol. 4, Iss. 6, pp. 778–791

doi: 10.1049/iet-map.2009.0057

cross-polarised components, $\mathcal{R}_{\iota\kappa}^{\iota'\kappa'} = \langle M_{\iota\kappa} M_{\iota'\kappa'}^{*} \rangle$

$$\mathcal{R}_{\iota\kappa}^{\iota'\kappa'} = 4\pi^2 \mathrm{i}^{l-l'-\lambda+\lambda'-\tau+\tau'+t-t'} \sum_{\alpha}\sum_{\beta} \iint \ldots A_{\iota,\alpha}^{*}(\hat{\boldsymbol{k}}_{\mathrm{r}}) A_{\iota',\alpha}(\hat{\boldsymbol{k}}_{\mathrm{r}}) \mathcal{P}_{\alpha\beta}(\hat{\boldsymbol{k}}_{\mathrm{r}}, \hat{\boldsymbol{k}}_{\mathrm{t}}) \ldots A_{\kappa,\beta}(\hat{\boldsymbol{k}}_{\mathrm{t}}) A_{\kappa',\beta}^{*}(\hat{\boldsymbol{k}}_{\mathrm{t}}) \, \mathrm{d}\Omega_{\mathrm{r}} \, \mathrm{d}\Omega_{\mathrm{t}} \quad (37)$$

Usually, the total power in the co-polarised and cross-polarised components satisfies the normalisation $P_{\theta\theta} + P_{\theta\phi} + P_{\phi\theta} + P_{\phi\phi} = 1$. Then normalisation of the total multipole power, $\sum_{\tau=1}^{2}\sum_{t=1}^{2}\sum_{m=-l}^{l}\sum_{\mu=-l}^{l}\sum_{l=1}^{L}\sum_{\lambda=1}^{L} P_{t\mu\lambda,\tau ml} = L^2(L+2)^2/8$, which directly follows from the addition theorem of spherical vector harmonics [12]. The derivation follows directly from the Gaussianity preservation property of affine transformations; details are given in Appendix D in [29].

As we can see from Proposition 1, the correlation depends on the joint distributions of co-polarised and cross-polarised components. Several well-known channels can be interpreted in the framework of this model. For example, if isotropic PAS is assumed at both the receiver and the transmitter

$$\mathcal{P}_{\alpha\beta}(\hat{\boldsymbol{k}}_{\mathrm{r}}, \hat{\boldsymbol{k}}_{\mathrm{t}}) = 1/16\pi^2 \quad (38)$$

we obtain that

$$\mathcal{R}_{\iota\kappa}^{\iota'\kappa'} = \delta_{tt'}\delta_{\mu\mu'}\delta_{\lambda\lambda'}\delta_{\tau\tau'}\delta_{mm'}\delta_{ll'} \quad (39)$$

Hence, all modes are uncorrelated in the isotropic case, this is the most random field that can be encountered in wireless channels. The covariance of the $\boldsymbol{H}$-matrix is then

$$\mathcal{R}_{ij}^{i'j'} = \sum_{\iota}\sum_{\kappa} R_{i\iota} R_{i',\iota}^{*} T_{\kappa j} T_{\kappa j'}^{*} \quad (40)$$

In this case, the correlation properties of the $\boldsymbol{H}$-matrix are, as we should expect, completely defined by the properties of the antennas used.

5 Numerical examples

The increasing demand for smaller devices for wireless communication has led to the search for methods to reduce the size of antennas in devices such as cellular phones. A well-known way to keep the volume occupied by antennas down, while still achieving or even increasing signal diversity, is to exploit polarisation diversity. Polarisation diversity has been the objective of extensive theoretical and practical studies, see [39] and references therein.

In the following example, we apply our approach to a MIMO system based on polarisation diversity. This example is an oversimplified antenna configuration that does not take mutual coupling or matching into account. However, it serves as a straightforward example demonstrating the main points in the paper. We consider a 2×2 MIMO system with cross-polarised antennas at both ends. Two half-wavelength dipoles are used, one is tilted 45° from the z-axis towards the positive side of the y-axis, while the second dipole is also tilted 45° but in the opposite direction. Thus we denote them as the $+45°$ dipole and the $-45°$ dipole, respectively (see Fig. 2). In order to illustrate how the multimode expansion can be used to analyse the interaction between the antennas and the channel, we rotate both antenna pairs around the x-axis, towards the positive y-axis, in their respective coordinate systems. The rotation angles are denoted by α_{r} and α_{t} for the receive and the transmit antenna pairs, respectively.

We denote the transfer function matrix, the $\boldsymbol{H}$-matrix, of the system by

$$\boldsymbol{H} = \begin{pmatrix} H_{++} & H_{+-} \\ H_{-+} & H_{--} \end{pmatrix} \quad (41)$$

where for instance, H_{+-} denotes the matrix element coupling the $+45°$ antenna at the receiver with the $-45°$ antenna at the transmitter. The notation of the remaining matrix elements follows the same principle. We keep the same notation for the rotated antennas.

The polarisation sensitivity of the multi-port antenna system as a function of the rotation angle can be directly derived from the behaviour of the multipoles. Fig. 3 shows the squared absolute values of the transmission (or reception) coefficients, (For clarity, the transmission coefficients in Fig. 3 are normalised as $\sum_{\iota}|R_{\iota}|^2 = 1$.) $|R_{\iota}|^2$, for the $+45°$-dipole and the $-45°$-dipole antennas as function of the rotation angle α for the six lowest multipole multi-indices, ι, that is, $l = 1$. As expected only the TM dipoles, that is, $l = 1$ and $\tau = 2$, are excited while the antennas are rotated. (From the properties of spherical functions, it follows that rotation conserves the power in the l-index and in the τ-index.) Their magnitudes clearly change, indicating that the coupling to the different modes changes as the antenna is rotated. For example, at the initial position, when $\alpha = 0°$, the positions of the

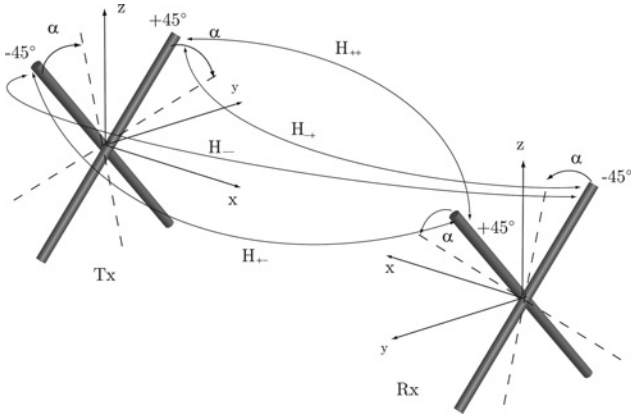

Figure 2 *Geometry of the cross-polarised MIMO system*

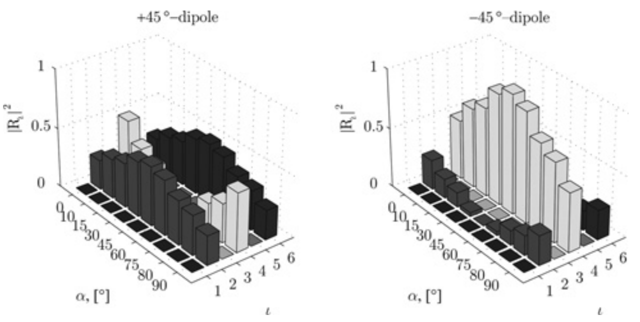

Figure 3 *Squared absolute values of the transmission (or reception) coefficients, $|R_\iota|^2$ of the half-wavelength dipole antenna tilted from $+45°$ to $+135°$ from the z-axis towards the y-axis (left plot) and the same but for tilting angles from $-45°$ to $+45°$ (right plot)*

$+45°$-dipole and the $-45°$-dipole antennas are equivalent because of symmetry and therefore the magnitudes of the multipoles are the same, with half of the power distributed equally between the two 'horizontal' dipole modes with $\iota = 2 \rightarrow \{2, -1, 1\}$ and $\iota = 6 \rightarrow \{2, 1, 1\}$. In this paper, we use the complex exponential convention of the spherical vector waves [12, 25]; therefore no distinct association between the actual physical orientation of the horizontal dipoles and the dipole order can be made. The other half of the power goes into the vertical dipole modes with $\iota = 4 \rightarrow \{2, 0, 1\}$. As we increase the rotation angle to $\alpha = 10°$ the tilt angle of the $+45°$ dipole increases to $55°$. At this angle the half-wavelength dipole senses powers in the horizontal and vertical polarisations in a similar manner [40]. In this case, the antenna coupling into the three dipole modes is equal as shown in the left plot of Fig. 3. Any further increase of the rotation angle implies an increase of the power into the 'horizontal' dipoles with the proportional decrease of the power into the 'vertical' dipole, which reaches their respective maxima and minimum for $\alpha = 45°$. On the contrary, for the $-45°$ dipole, as the rotation angle increases, the power coupled into the 'vertical' dipole increases, while the power into the 'horizontal' dipoles decreases. Owing to symmetry the reverse process is observed as the rotation angle is increased towards $\alpha = 90°$.

The correlation between the two antenna branches can also be explained from the multipole behaviour. For example, for $\alpha = 0°$, the correlation between the two antennas should be the highest since, as explained earlier, both antennas excite the same modes equally. On the other hand, for $\alpha = 45°$, the two antennas are 'purely orthogonal' since they excite orthogonal modes, that is, one antenna, the $+45°$ dipole, is oriented along the y-axis, hence only 'horizontal' dipoles are excited while the other antenna is oriented along the z-axis.

We now proceed to specify the channel models we use for the analysis of the MIMO system. It is well known that an antenna performs differently depending on the propagation environment where it is deployed. Thus, if we by some means can gain knowledge of the properties of the propagation channel we can, in principle, improve the performance in that channel by reconfiguring the antenna so that it matches the channel characteristics. Here we are, however, just going to analyse the performance to illustrate how well (or badly) our simple system performs in terms of the properties of the channel $\boldsymbol{H}$-matrix and how the channel properties depend upon the interaction between the multipoles of the antenna and that of the channel.

We consider two simple but widely used models. In both of them it is assumed that the joint probability density functions are the same for both co-polarised and cross-polarised components, and that they are independent in azimuth and elevation

$$p_{\alpha\beta}(\theta_r, \phi_r, \theta_t, \phi_t) = p_{\theta_r\alpha\beta}(\theta_r)p_{\phi_r\alpha\beta}(\phi_r)p_{\theta_t\alpha\beta}(\theta_t)p_{\phi_t\alpha\beta}(\phi_t) \tag{42}$$

where $\alpha = \{\theta, \phi\}$ and $\beta = \{\theta, \phi\}$ stands for either of $\hat{\boldsymbol{\theta}}$ or $\hat{\boldsymbol{\phi}}$ polarisations. We also assume that the powers of the cross-polarised components are much lower than the powers of the co-polarised components, that is, $P_{\theta\phi} \simeq P_{\phi\theta} \ll P_{\theta\theta}, P_{\phi\phi}$ and therefore the XPR is completely defined by $\chi = P_{\theta\theta}/P_{\phi\phi}$.

Model A describes a highly isotropic channel with a balanced polarisation ($\chi = 0$ dB), where

$$p_{\theta_r\alpha\beta}(\theta) = p_{\theta_t\alpha\beta}(\theta) = A_\theta\, \mathrm{e}^{-\sqrt{2}|\theta-\mu_\theta|/\sigma_\theta} \sin\theta, \quad \theta \in [0, \pi] \tag{43}$$

$$p_{\phi_r\alpha\beta}(\phi) = p_{\phi_t\alpha\beta}(\phi) = A_\phi\, \mathrm{e}^{-\sqrt{2}|\phi-\mu_\phi|/\sigma_\phi}, \quad \phi \in [-\pi, \pi) \tag{44}$$

where $A_\theta = 0.541$ and $A_\phi = 0.197$ computed with parameters $\sigma = \sigma_\theta = \sigma_\phi = 10$ rad, $\mu_\theta = \pi/2$ and $\mu_\phi = 0$ rad.

Model B emulates the propagation in a macro-cell deployed in an urban environment as outlined in [10]. Here we use the shape of the distributions provided in [10]. However, the parametrisation is generic. We assume that

$$p_{\theta_r\alpha\beta}(\theta) = \sqrt{2}\sin\theta, \ \theta \in \left[\frac{\pi}{4}, \frac{\pi}{2}\right] \tag{45}$$

$$p_{\phi_r\alpha\beta}(\phi) = \frac{1}{2\pi}, \ \phi \in [-\pi, \pi) \tag{46}$$

$$p_{\theta_t\alpha\beta}(\theta) = A_\theta\, \mathrm{e}^{-\sqrt{2}|\theta-\mu_\theta|/\sigma_\theta} \sin\theta, \quad \theta \in [0, \pi] \tag{47}$$

$$p_{\phi_t\alpha\beta}(\phi) = A_\phi\, \mathrm{e}^{-\sqrt{2}|\phi-\mu_\phi|/\sigma_\phi}, \quad \phi \in [-\pi, \pi) \tag{48}$$

where $A_\theta = 7.106$ and $A_\phi = 7.071$ computed with parameters $\sigma = \sigma_\theta = \sigma_\phi = 0.1$ rad and $\mu_\theta = \pi/2$ and $\mu_\phi = 0$ rad. We also assume unbalanced polarisation in favour to the vertical polarisation, that is, $\chi = 10$ dB. Here the mobile terminal is the receiver, whereas the transmitter is the base station.

doi: 10.1049/iet-map.2009.0057

Hence, the angle-spread around the Rx is much higher than the angle-spread around the Tx.

In both models the resulting channels produce a Rayleigh probability density function for the envelopes of the elements of the $\boldsymbol{H}$-matrix.

Figs. 4 and 5 show the average mode-to-mode power, $\langle|M_{\iota\kappa}|^2\rangle$, as a function of the multipole indices at the Rx, ι and the Tx, κ, for Model A and Model B, respectively. The more uniform distribution of the power among the multimodes of Model A is a direct result of the uniform distribution of the AoA and the AoD at the receiver and the transmitter, respectively. The fact that the power into the vertical and horizontal polarisations is the same, also supports this uniform power distribution among the modes. On the other hand, spatial selectivity, as we have at the transmitter for Model B, together with polarisation power imbalance also implies selectivity in modes, that is, some multipole–multipole interactions are stronger than others as shown in Fig. 5. More specifically, we see from Fig. 5 that the coupling between the power into the 'vertical' dipole modes, $\iota = \kappa = 4 \rightarrow \{2, 0, 1\}$, is much stronger than the power coupling between other modes, since the XPR of the channel is such that the power into the power of the vertical polarisation is much stronger than the power of the horizontal polarisation, $\chi = 10$ dB. It can also be observed that the coupling between electric and magnetic dipoles is quite strong since the propagation at the receiver takes place mostly on the horizontal plane.

Figs. 6 and 7 show the absolute values of the correlation matrix, $|R_{\iota\kappa}|$, as function of the multipole indices at the receiver, (ι, κ), and the transmitter, (ι', κ'), for Model A and Model B, respectively. The index pair (ι, κ) denotes a multi-index calculated as $\boldsymbol{\iota} \otimes \boldsymbol{\kappa}$, where $\otimes$ denotes the Kronecker product. As we see from Fig. 6, the multimodes become uncorrelated in the case of a uniform distribution of AoA and AoD, whereas the correlation becomes noticeably higher for the spatially selective channel provided by Model B. It should be noted that in the case when the power of co-polarised and cross-polarised components is the same, that is, $P_{\theta\phi} = P_{\phi\theta} = P_{\theta\theta} = P_{\phi\phi} = 1/4$ and the joint pdf of the AoA and AoD is uniform, that is, $p_{\theta\theta}(\Omega_r, \Omega_t) = p_{\theta\phi}(\Omega_r, \Omega_t) = p_{\phi\theta}(\Omega_r, \Omega_t) = p_{\phi\phi}(\Omega_r, \Omega_t) = 1/16\pi^2$, the multimodes have identical powers given by the diagonal elements of (39).

The channel behaviour in the multipole modes, that is, the $\boldsymbol{M}$-matrix, together with the mode behaviour of the antennas,

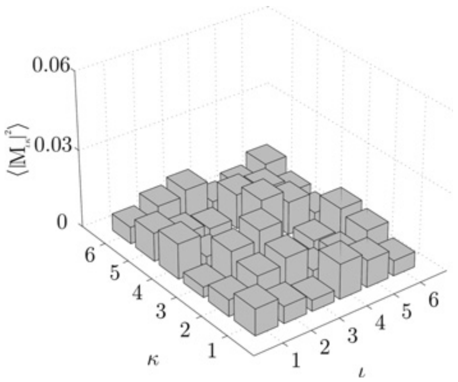

Figure 4 *Average mode to mode power, $\langle|M_{\iota\kappa}|^2\rangle$, as function of the multipole indices at the receiver, ι, and the transmitter, κ, for Model A*

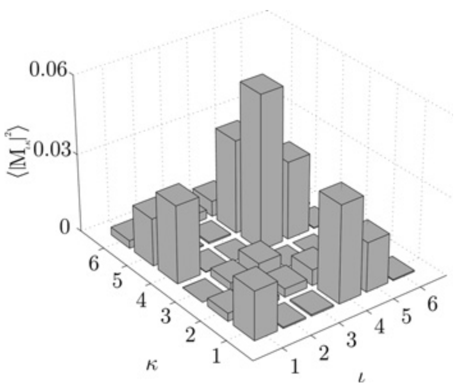

Figure 5 *Average power mode, $\langle|M_{\iota\kappa}|^2\rangle$ as function of the multipole indices at the receiver, ι, and the transmitter, κ, for Model B*

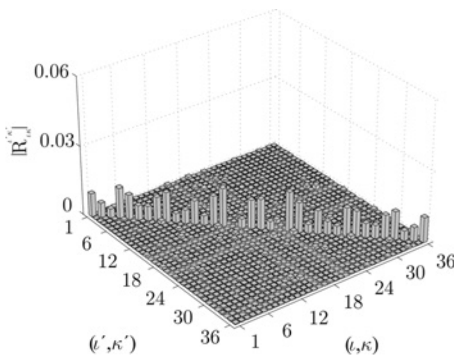

Figure 6 *Absolute value of the covariance matrix, $|R_{\iota\kappa}|$, as function of the multipole indices at the receiver, (ι, κ), and the transmitter, (ι', κ'), for Model A*

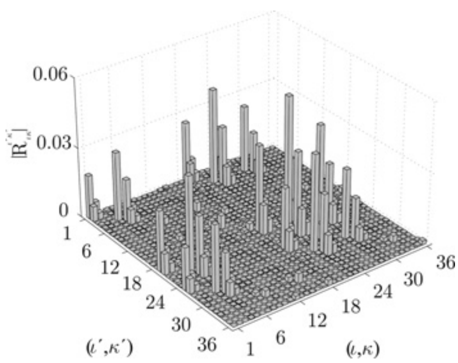

Figure 7 *Absolute value of the covariance matrix, $|R_{\iota\kappa}|$, as function of the multipole indices at the receiver, (ι, κ), and the transmitter, (ι', κ'), for Model B*

given by the transmission and reception matrices $\boldsymbol{R}$ and $\boldsymbol{T}$, have direct impact on the behaviour of the $\boldsymbol{H}$-matrix. Fig. 8 shows the average power of the elements of the 2×2 $\boldsymbol{H}$-matrix as a function of the rotation angles at the receiver and the transmitter obtained using Model A. As we can see, the power is practically the same for all links and it does not depend on the rotation of the antennas. On the other hand, similar results obtained using Model B show how the XPR and spatial selectivity (and therefore selectivity in modes too) impact the link power. For both Model A and Model B the powers of the links H_{+-} and H_{-+} are mutually symmetric and symmetric with respect to the rotation angle α. On the other hand, the powers of the links H_{++} and H_{--} are not mutually symmetric, although each of them is symmetric with respect to the rotation angle α (Fig. 9). Clearly, the link is strongest for the H_{--} link in Model B since both antennas are collinear and their polarisations coincide with the polarisation of the channel (see Figs. 3 and 5 for a comparison).

The correlation coefficients of the $\boldsymbol{H}$-matrix are shown in Figs. 10 and 11, for Model A and Model B, respectively. As anticipated by the mode correlation in Fig. 7, the correlation coefficient is low for Model A as shown in Fig. 10. Here, we also observe a symmetric behaviour for the corresponding links. Moreover, we see that for the isotropic channel discussed above the covariance is only determined by the antennas, see (40). On the other hand, the correlation increases considerably with spatial selectivity as in Model B, shown in Fig. 11. Also here, the behaviour can be anticipated by the covariance of the multimodes observed in Fig. 7. The asymmetrical behaviour of the correlation coefficients is explained by the asymmetry in AoA and AoD as well as the power polarisation imbalance.

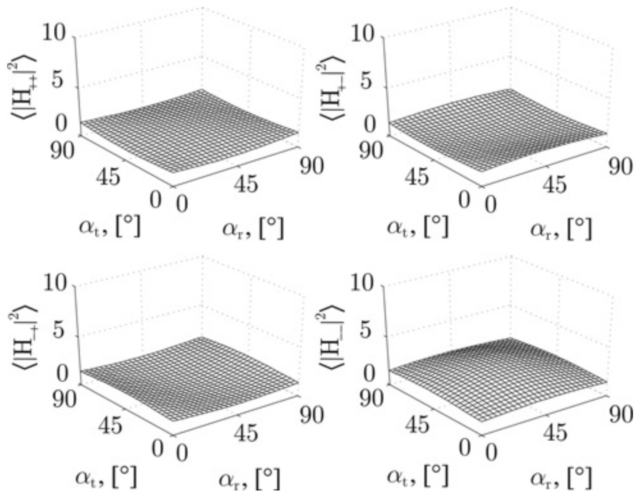

Figure 8 *Average power of the elements of the* 2×2 ***H****-matrix as a function of the rotation angles at the receiver and the transmitter, Model A*

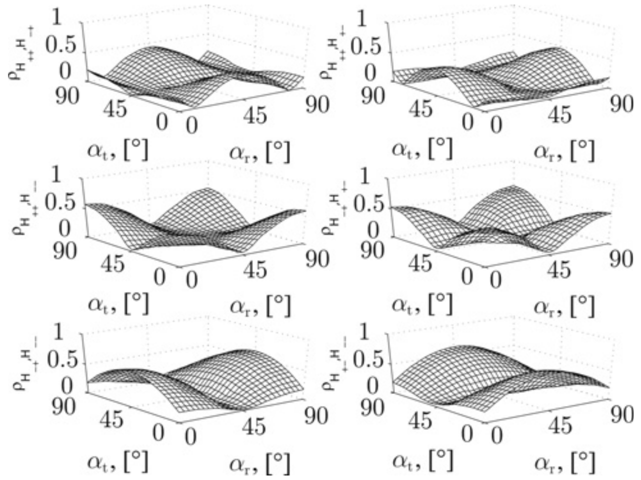

Figure 10 *Correlation coefficients between pairs of elements of the* 2×2 ***H****-matrix as a function of the rotation angles at the receiver and the transmitter, Model A*

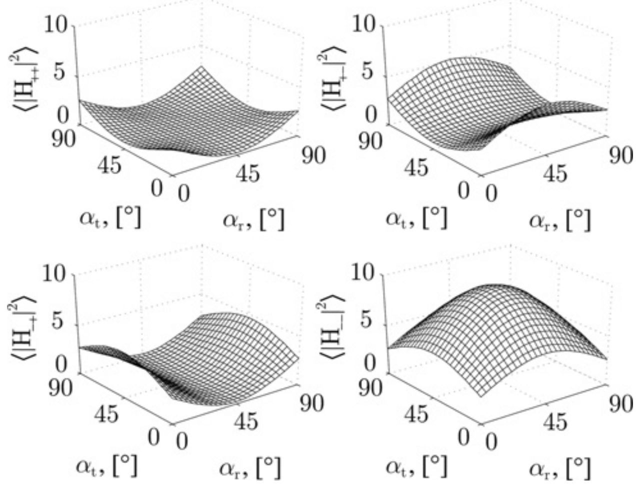

Figure 9 *Average power of the elements of the* 2×2 ***H****-matrix as a function of the rotation angles at the receiver and the transmitter, Model B*

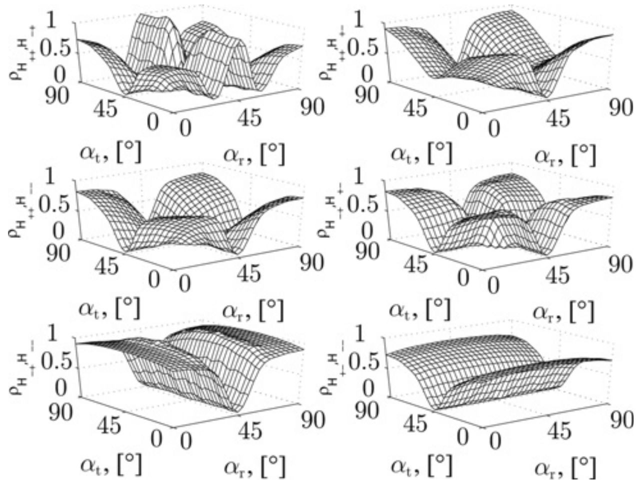

Figure 11 *Correlation coefficients between pairs of elements of the* 2×2 ***H****-matrix as a function of the rotation angles at the receiver and the transmitter, Model B*

IET Microw. Antennas Propag., 2010, Vol. 4, Iss. 6, pp. 778–791
doi: 10.1049/iet-map.2009.0057

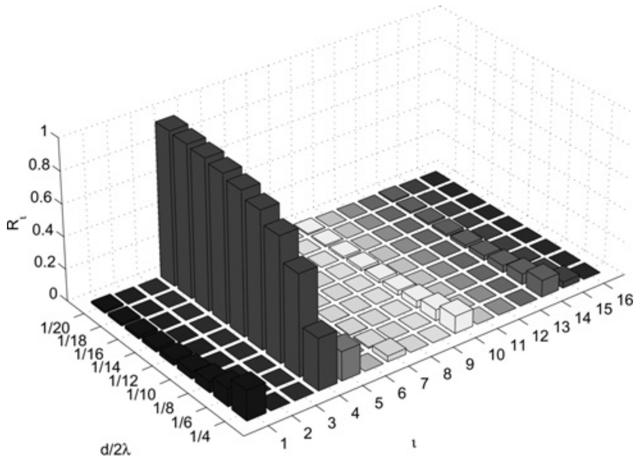

Figure 12 *Squared absolute values of the transmission (or reception) coefficients,* $|R_\iota|^2$ *of one of the vertically polarised half-wavelength dipole antenna elements as a function of the offset distance from a reference coordinate system. It is assumed that there is no mutual coupling between the antennas*

As a final remark, we would like to briefly mention spatial-diversity systems, which draw special attention in the design of MIMO wireless systems. The topic of spatial diversity has been thoroughly analysed since the seminal work presented in [41]. Spatial diversity has proven to have a great impact on wireless communications systems both through increased transmission rates and/or increased reliability (lower error probability) [31]. A system of particular interest, because of its 'apparent' simplicity, is the 2×2 MIMO spatial-diversity system with half-wavelength dipoles placed at some distance d_s from each other. Here we show a short example when varying d_s. The squared absolute values of the transmission (or reception) coefficients, $|R_\iota|^2$ of a vertically polarised half-wavelength dipole antenna as a function of the offset distance from a reference coordinate system, $2d_s/\lambda$, is given in Fig. 12 (compare with Fig. 3). A similar behaviour is observed for the second antenna too. As can be seen from the plot, the translation of the antenna is equivalent to the excitation of higher order multipoles, for example, coefficients with multipole index $l = 2$ have to be taken into the analysis of the interaction between the antenna and the channel for a separation as low as $\lambda/2$. This 'spread' in modes can be seen as the origin of the low correlation between spatially separated antenna branches. For more compact configurations, for example, $d_s \leq \lambda/6$, the representation of the antenna is mainly concentrated to coefficients corresponding to dipole modes ($l = 1$), more specifically to the 'vertical' dipole moment with $\iota = 4$. Therefore the correlation of closely placed dipoles is high unless 'intelligent' matching measures are taken [20, 42, 43].

6 Summary

In this paper, we introduced the concept of mode-to-mode channel matrix, the $\boldsymbol{M}$-matrix, to describe the coupling between the spherical vector wave modes excited at the transmitter to the modes excited at the receiver of a wireless MIMO system. The $\boldsymbol{M}$-matrix contains all relevant information about the physics involving the excitation of the channel by electromagnetic waves, since it provide a direct coupling among different multipoles at the receiver and the transmitter. We further discussed the concept of the channel scattering dyadic, $\boldsymbol{\mathcal{C}}$, which maps the field radiated by the transmitting antenna to the field impinging at the receive antenna obtained by superposition of plane waves. Further, using the correlation model for the amplitudes incident at the receive antenna [10], we developed a more general correlation model for the double-directional channel, that is, the correlation between the co-polarised and cross-polarised components of the channel scattering dyadic. We then expanded the channel $\boldsymbol{H}$-matrix in spherical vector wave modes using the derived correlation model for the elements of the channel scattering dyadic. We also provided results for first- and second-order statistics of the expansion coefficients based on the assumption that the dyadic elements are independently distributed Gaussian variables. The equations we proved establish direct relationship between the elements of $\boldsymbol{H}$ and $\boldsymbol{M}$, and therefore the spatial, directional and polarisation properties of the channel and the antennas for MIMO systems.

Our results can be used to further analyse the interaction between the antennas and the channel and the performance limits of antennas in stochastic channels. Further investigations of the behaviour of the mode-to-mode channel matrix should also enable valuable insights into design of small and efficient MIMO antenna arrays.

7 Acknowledgment

This work was supported financially by SSF Center of Excellence for High Speed Wireless Communications.

8 References

[1] WINTERS J.H.: 'On the capacity of radio communications systems with diversity in Rayleigh fading environments', *IEEE J. Sel. Areas Commun.*, 1987, **5**, pp. 871–878

[2] FOSCHINI G.J., GANS M.J.: 'On limits of wireless communications in a fading environment when using multiple antennas', *Wirel. Pers. Commun.*, 1998, **6**, pp. 311–335

[3] TELATAR E.: 'Capacity of multi-antenna Gaussian channels', *Eur. Trans. Telecommun.*, 1999, **10**, (6), pp. 585–595

[4] TAROKH V., SESHDARI N., CALDERBANK A.R.: 'Space–time codes for high data rate wireless communication: performance criterion and code construction.', *IEEE Trans. Inf. Theory*, 1998, **44**, (2), pp. 744–765

[5] PAULRAJ A., NABAR R., GORE D.: 'Introduction to space–time wireless communications' (Cambridge University Press, New York, NY, USA, 2003)

[6] BIGLIERI E., CALDERBANK R., CONSTANTINIDES A., GOLDSMITH A., PAULRAJ A., POOR H.V.: 'MIMO wireless communications' (Cambridge University Press, New York, NY, USA, 2007)

[7] STEINBAUER M., MOLISCH A.F., BONEK E.: 'The double-directional radio channel', *IEEE Antennas Propag. Mag.*, 2001, **43**, pp. 51–63

[8] XU H., CHIZHIK D., HUANG H., VALENZUELA R.: 'A generalized space–time multiple-input multiple-output (MIMO) channel model', *IEEE Trans. Wirel. Commun.*, 2004, **3**, pp. 966–975

[9] GLAZUNOV A.A.: 'Mean effective gain of user equipment antennas in double directional channels'. 15th IEEE Int. Symp. on Personal, Indoor and Mobile Radio Communications, 2004 (PIMRC 2004), September 2004, vol. 1, pp. 432–436

[10] CORREIA L. (ED.): 'COST 273 final report: towards mobile broadband multimedia networks' (Elsevier, 2006)

[11] HANSEN W.W.: 'A new type of expansion in radiating problems', *Phys. Rev.*, 1935, **47**, pp. 139–143

[12] HANSEN J.E. (ED.): 'Spherical near-field antenna measurements' (Peter Peregrinus, London, UK, 1988)

[13] LEWIS R.: 'Spherical-wave source-scattering matrix analysis of coupled antennas; a general system two-port solution', *IEEE Trans. Antennas Propag.*, 1987, **35**, pp. 1375–1380

[14] GLAZUNOV A.A., GUSTAFSSON M., MOLISCH A.F., TUFVESSON F., KRISTENSSON G.: 'Spherical vector wave expansion of gaussian electromagnetic fields for antenna–channel interaction analysis', *IEEE Trans. Antennas Propag.*, 2009, **57**, (7), pp. 2055–2067

[15] SVANTESSON T.: 'An antenna solution for MIMO channels: the multimode antenna'. Conf. Record of the 34th Asilomar Conf. on Signals, Systems and Computers, 29 October–1 November 2000, vol. 2, pp. 1617–1621

[16] SVANTESSON T.: 'On the potential of multimode antenna diversity'. 52nd IEEE VTS-Fall Vehicular Technology Conf., 2000 (VTC 2000), 24–28 September 2000, vol. 5, pp. 2368–2372

[17] POLLOCK T.S., ABHAYAPALA T.D., KENNEDY R.A.: 'Introducing space into MIMO capacity calculations', *J. Telecommun. Syst.*, 2003, **24**, (2), pp. 415–436

[18] POLLOCK T., ABHAYAPALA T., KENNEDY R.: 'Spatial limits to MIMO capacity in general scattering environments'. Seventh Int. Symp. on DSP for Communication Systems, pp. 49–54

[19] LOYKA S.: 'Information theory and electromagnetism: are they related?'. Int. Symp. on Antenna Technology and Applied Electromagnetics (ANTEM'04), 20–23 July 2004

[20] JENSEN J., WALLACE M.A.: 'A review of antennas and propagation for MIMO wireless communications', *IEEE Trans. Antennas Propag.*, 2004, **52**, (11), pp. 2810–2824

[21] HANLEN L., FU M.: 'Wireless communication systems with-spatial diversity: a volumetric model', *IEEE Trans. Wirel. Commun.*, 2006, **5**, pp. 133–142

[22] HANLEN L.W., TIMO R.C.: 'Intrinsic capacity of random scattered spatial communication'. IEEE Information Theory Workshop, 2006 (ITW'06), Chengdu, October 2006, pp. 281–285

[23] MIGLIORE M.: 'An intuitive electromagnetic approach to MIMO communication systems', *IEEE Antennas Propag. Mag.*, 2006, **48**, (3), pp. 128–137

[24] KLEMP O., EUL H.: 'Radiation pattern analysis of antenna systems for MIMO and diversity configurations', *Adv. Radio Sci.*, 2005, **3**, pp. 157–165

[25] GUSTAFSSON M., NORDEBO S.: 'Characterisation of MIMO antennas using spherical vector waves', *IEEE Trans. Antennas Propag.*, 2006, **54**, pp. 2679–2682

[26] GUSTAFSSON M., NORDEBO S.: 'On the spectral efficiency of a sphere', *Prog. Electromagn. Res.*, 2007, **PIER 67**, pp. 275–296

[27] NORDEBO S., GUSTAFSSON M., KRISTENSSON G.: 'On the capacity of the free space antenna channel'. IEEE Antennas and Propagation Society Int. Symp. 2006, 9–14 July 2006, pp. 3105–3108

[28] SVANTESSON T.: 'A physical MIMO radio channel model for multi-element multi-polarized antenna systems'. 54th IEEE VTS Fall Vehicular Technology Conf. 2001 (VTC 2001), 7–11 October 2001, vol. 2, pp. 1083–1087

[29] GLAZUNOV A.A., GUSTAFSSON M., MOLISCH A.F., TUFVESSON F.: 'Physical modeling of MIMO antennas and channels by means of the spherical vector wave expansion'. Technical Report LUTEDX/(TEAT-7177)/1–31/(2009), Faculty of Engineering, Department of Electrical and Information Technology, LTH, Lund University, Lund, Sweden, 2009. Available at: http://www.eit.lth.se

[30] BELLO P.A.: 'Characterization of randomly time-variant linear channels', *IEEE Trans. Commun. Syst.*, 1963, **11**, pp. 360–393

[31] MOLISCH A.F.: 'Wireless communications' (IEEE Press, Wiley, 2005)

doi: 10.1049/iet-map.2009.0057

[32] CORREIA L. (ED.): 'COST 259 final report: wireless flexible personalised communications' (Wiley, 2001)

[33] CZINK N., CERA P., SALO J., BONEK E., YLITALO J., NUUTINEN J.-P.: 'A framework for automatic clustering of parametric MIMO channel data including path powers'. VTC 2006 – Fall, September 2006

[34] PAPOULIS A.: 'Probability, random variables and stochastic processes' (Mc Graw-Hill International Edition, 1991)

[35] STEINBAUER M., HAMPICKE D., SOMMERKORN G., SCHNEIDER A., MOLISCH A.F., THOMAE R., BONEK E.: 'Array measurement of the double-directional mobile radio channel'. Proc. IEEE Vehicular Technology Conf. on Spring 2000, 2000

[36] BONEK E., STEINBAUER M.: 'Double-directional channel measurements'. Proc. Int. Conf. on Antennas Propagation 2001, 2001, pp. 226–230

[37] KATTENBACH R.: 'Statistical modeling of small-scale fading in directional radio channels', *IEEE J. Sel. Areas Commun.*, 2002, **20**, (3), pp. 584–592

[38] FLEURY B.H.: 'First- and second-order characterization of direction dispersion and space selectivity in the radio channel', *IEEE Trans. Inf. Theory*, 2000, **46**, pp. 2027–2044

[39] VAUGHAN R., ANDERSEN J.B.: 'Channels, propagation and antennas for mobile communications' (IEE Press, 2003, 1st edn.)

[40] TAGA T.: 'Analysis for mean effective gain of mobile antennas in land mobile radio environments', *IEEE Trans. Veh. Technol.*, 1990, **39**, pp. 117–131

[41] LEE W.C.Y.: 'Antenna spacing requirement for a mobile radio base-station diversity', *Bell Syst. Tech. J.*, 1971, **50**, pp. 1859–1876

[42] WALLACE J., JENSEN M.: 'Termination-dependent diversity performance of coupled antennas: network theory analysis', *IEEE Trans. Antennas Propag.*, 2004, **52**, pp. 98–105

[43] ANDERSEN J.B., LAU B.K.: 'On closely coupled dipoles in a random field', *IEEE Trans. Antennas Wirel. Propag. Lett.*, 2006, **5**, (1), pp. 73–75